

Atomic parity nonconservation in Ra^+

L. W. Wansbeek, B. K. Sahoo, R. G. E. Timmermans*, and K. Jungmann
 KVI, University of Groningen, NL-9747 AA Groningen, The Netherlands

B. P. Das

Non-accelerator Particle Physics Group, Indian Institute of Astrophysics, Bangalore-560034, India

D. Mukherjee

Department of Physical Chemistry, Indian Association for Cultivation of Science, IACS, Kolkata 70032, India and
 Raman Center for Atomic, Molecular and Optical Sciences, IACS, Kolkata 70032, India

(Dated: November 11, 2021)

We report on a theoretical analysis of the suitability of the $7s^2S_{1/2} \leftrightarrow 6d^2D_{3/2}$ transition in singly ionized radium to measure parity nonconservation, in the light of an experiment planned at the KVI of the University of Groningen. Relativistic coupled-cluster theory has been employed to perform an *ab initio* calculation of the parity nonconserving electric dipole amplitude of this transition, including single, double, and leading triple excitations. We discuss the prospects for a sub-1% precision test of the electroweak theory of particle physics.

In atomic systems, parity is broken due to the exchange of the neutral vector boson Z^0 , which mediates the weak interaction between the atomic electrons and the quarks in the nucleus. This atomic parity nonconservation (APNC) gives rise to small parity nonconserving electric dipole transition amplitudes ($E1_{\text{PNC}}$). The APNC effect gets strongly enhanced in heavy atoms and can be measured by the interference of $E1_{\text{PNC}}$ with a suppressed electromagnetic transition amplitude ($M1$, $E2$) [1, 2]. The accurate measurement of the $6s^2S_{1/2} \leftrightarrow 7s^2S_{1/2}$ transition in atomic ^{133}Cs by the Boulder group [3, 4] constitutes a precision test of the electroweak sector of the Standard Model (SM) of particle physics [5]. By combining the measurement with a many-body atomic structure calculation, the weak nuclear charge could be determined [6].

The importance of APNC to particle physics is a strong incentive to further pursue these challenging experiments. With the experimental and theoretical accuracies at an impressive 0.35% [3, 4] and 0.5% [6] level, respectively, the ^{133}Cs result agrees with the SM prediction within one standard deviation. Nevertheless, it is desirable to consider other candidates for APNC studies, see *e.g.* Ref. [7]. New experiments have been proposed for Cs [8] and Fr [9] atoms. Of special interest is the proposal by Fortson to measure APNC in *one single* laser-cooled and trapped ion [2]. Such single-ion experiments offer important benefits, such as long coherence times and precise control of various systematic effects. Promising ions from the experimental and atomic-theory point of view are heavy alkali-like ions, in particular Ba^+ and Ra^+ [10]. Proof-of-principle experiments have been carried out with $^{138}\text{Ba}^+$ by the Fortson group [10, 11, 12].

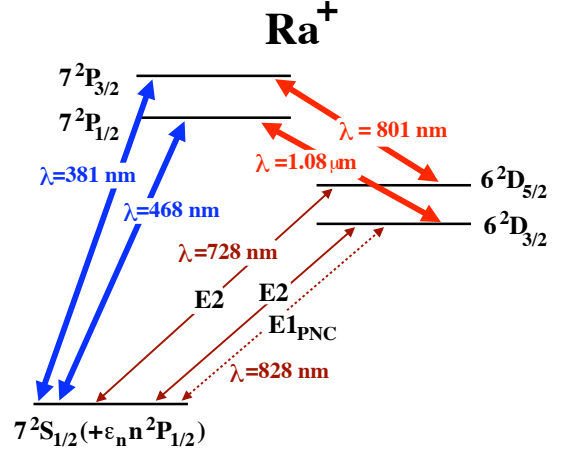


FIG. 1: Relevant energy levels in Ra^+ .

At the TRI μ P facility [13, 14] at the accelerator institute KVI in Groningen an APNC experiment on Ra^+ is in progress [15]. An important advantage of Ra^+ is that all relevant transitions are in the optical regime, *cf.* Fig. 1, and thus are accessible by commercially available solid-state laser technology. The goal is to measure the $E1_{\text{PNC}}$ amplitude of the $7s^2S_{1/2} \leftrightarrow 6d^2D_{3/2}$ transition. We address here the question what the prospects are to push the corresponding atomic theory below 1%, such that the experiment can serve as a high-precision test of the SM. We analyze various relevant properties of Ra^+ and assess the remaining uncertainties.

The parity-nonconserving nuclear-spin independent (NSI) interaction is due to the electron-quark neutral weak interaction, the Hamiltonian of which is given by

$$H_{\text{PNC}}^{\text{NSI}} = \frac{G_F}{2\sqrt{2}} Q_W \gamma_5 \varrho_{\text{nuc}}(r), \quad (1)$$

where G_F is the Fermi constant, ϱ_{nuc} the nuclear density,

*Electronic address: timmermans@kvi.nl

and γ_5 is the standard Dirac matrix; Q_W is the weak nuclear charge, which is equal to $(2Z + N)c_{1u} + (2N + Z)c_{1d}$ in terms of the coupling constants of the electron to the up and down quarks; Z and N are the number of protons and neutrons. The Hamiltonian in Eq. (1) mixes atomic states of opposite parity but with the same angular momentum. Its strength is weak enough to consider it as a first-order perturbation. We therefore write the valence state (v) atomic wave function as

$$|\Psi_v\rangle = |\Psi_v^{(0)}\rangle + G_F |\Psi_v^{(1)}\rangle, \quad (2)$$

where $|\Psi_v^{(0)}\rangle$ is the atomic wave function of the Dirac-Coulomb (DC) Hamiltonian (H_{DC}) and $|\Psi_v^{(1)}\rangle$ is the first-order correction due to the PNC NSI interaction.

To a first-order approximation, the $E1_{\text{PNC}}$ transition amplitude between the $7s^2S_{1/2}$ ($= i$) and $6d^2D_{3/2}$ ($= f$) states is given by

$$E1_{\text{PNC}} = G_F \frac{\langle \Psi_f^{(0)} | D | \Psi_i^{(1)} \rangle + \langle \Psi_f^{(1)} | D | \Psi_i^{(0)} \rangle}{\sqrt{\langle \Psi_f^{(0)} | \Psi_f^{(0)} \rangle \langle \Psi_i^{(0)} | \Psi_i^{(0)} \rangle}}, \quad (3)$$

which, after expansion, takes the form

$$E1_{\text{PNC}} = \sum_{I \neq i} \frac{\langle \Psi_f^{(0)} | D | \Psi_I^{(0)} \rangle \langle \Psi_I^{(0)} | H_{\text{PNC}}^{\text{NSI}} | \Psi_i^{(0)} \rangle}{(E_i - E_I) \sqrt{\langle \Psi_f^{(0)} | \Psi_f^{(0)} \rangle \langle \Psi_i^{(0)} | \Psi_i^{(0)} \rangle}} + \sum_{J \neq f} \frac{\langle \Psi_f^{(0)} | H_{\text{PNC}}^{\text{NSI}} | \Psi_J^{(0)} \rangle \langle \Psi_J^{(0)} | D | \Psi_i^{(0)} \rangle}{(E_f - E_J) \sqrt{\langle \Psi_f^{(0)} | \Psi_f^{(0)} \rangle \langle \Psi_i^{(0)} | \Psi_i^{(0)} \rangle}}, \quad (4)$$

where D is the electric dipole ($E1$) operator, I and J represent the allowed intermediate states, and E is the energy of the state. An accurate determination of $E1_{\text{PNC}}$ depends on the precision of the matrix elements of D and of $H_{\text{PNC}}^{\text{NSI}}$, and of the energy differences between the different states. At the same time, it is also important to take all intermediate states into account, something which is not possible in the often-used sum-over-states approach. We therefore employ the relativistic coupled-cluster (RCC) theory, which allows us to evaluate the properties to all orders in perturbation theory. The RCC method was previously used to calculate APNC in $^{137}\text{Ba}^+$ with sub-1% accuracy [16].

We obtain the first-order wave functions of Eq. (3) in the RCC framework as the solution of

$$G_F (H_{\text{DC}} - E_v) |\Psi_v^{(1)}\rangle = -H_{\text{PNC}}^{\text{NSI}} |\Psi_v^{(0)}\rangle, \quad (5)$$

where v stands for valence electron, which is either i or f . The unperturbed and perturbed wave functions are expressed as

$$|\Psi_v^{(0)}\rangle = \exp(T^{(0)}) \{1 + S_v^{(0)}\} |\Phi_v\rangle, \quad (6)$$

and

$$\begin{aligned} |\Psi_v^{(1)}\rangle &= \exp(T') \{1 + S_v'\} |\Phi_v\rangle \\ &= \exp(T^{(0)}) (T^{(1)} \{1 + S_v^{(0)}\} + \{S_v^{(1)}\}) |\Phi_v\rangle, \end{aligned} \quad (7)$$

respectively, where $|\Phi_v\rangle$ is the mean-field wave function determined with the Dirac-Fock (DF) method. T and S_v are the core and valence-core RCC correlation operators, respectively, where the superscript 0 indicates in the presence of the Coulomb interaction, the prime ($'$) indicates in the presence of both the Coulomb and APNC interaction, and 1 indicates their linear approximations. Substituting the above expressions in Eq. (3), we obtain

$$E1_{\text{PNC}} = G_F \frac{\langle \Phi_f | C_f^\dagger \overline{D^{(0)}} C_i | \Phi_i \rangle}{\sqrt{(1 + N_f^{(0)})(1 + N_i^{(0)})}}, \quad (8)$$

where

$$\begin{aligned} N_v^{(0)} &= \langle \Phi_v | S_v^{(0)\dagger} \exp(T^{(0)\dagger}) \exp(T^{(0)}) S_v^{(0)} | \Phi_v \rangle, \quad (9) \\ C_v &= T^{(1)} \{1 + S_v^{(0)}\} + S_v^{(1)}, \quad (10) \end{aligned}$$

and $\overline{D^{(0)}} = \exp(T^{(0)\dagger}) D \exp(T^{(0)})$. The matrix element is evaluated using the generalized Wick's theorem [16].

Our RCC work has two salient features. We evaluate $E1_{\text{PNC}}$ by using the direct solution of the first-order perturbed equation as given in Eq. (5) rather than summing over a finite number of intermediate states [17]. The core correlation effects modified by the parity nonconserving weak interaction are evaluated to all orders through $T^{(1)}$ in the framework of the relativistic CCSD(T) method. These effects cancel strongly in Cs and Fr, where both the initial and final states are S -states. However, it is essential to consider them accurately in the S - D transitions in Ba^+ and Ra^+ , where these contributions are significant. For our calculation, we have used numerical DF/ V^{N-1} orbitals to describe the occupied and bound virtual orbitals. The continuum states were represented by V^{N-1} Gaussian-type orbitals (GTOs) [18] using the parameters $\alpha = 5.25 \times 10^{-3}$ and $\beta = 2.73$. The finite size of the nucleus is accounted for by assuming a Fermi charge distribution [18].

In Table I, we present our RCC results for the $E1_{\text{PNC}}$ amplitude of the $7s^2S_{1/2} \leftrightarrow 6d^2D_{3/2}$ transition in the isotope $^{226}\text{Ra}^+$. Shown are the results of the DF method, of the RCC method with single and double excitations (CCSD), and with the leading triple excitations (CCSD(T)). The difference between the CCSD(T) and CCSD results is small. Our best value is the CCSD(T) result $E1_{\text{PNC}} = 46.4 \times 10^{-11} iea_0 (-Q_W/N)$. Also shown are two results of Dzuba *et al.* [19]: in a sum-over-states

TABLE I: $E1_{\text{PNC}}$ for the $7s^2S_{1/2} \leftrightarrow 6d^2D_{3/2}$ transition in the isotope $^{226}\text{Ra}^+$, in units of $10^{-11} iea_0 (-Q_W/N)$.

| | <i>This work</i> | Ref. [19] |
|---------|------------------|----------------------|
| DF | 40.4 | |
| CCSD | 46.1 | Mixed-states 42.9 |
| CCSD(T) | 46.4 | Sum-over-states 45.9 |

approach they found $45.9 \times 10^{-11}iea_0(-Q_W/N)$; in a mixed-states approach, wherein the APNC interaction explicitly mixes states of opposite parity, they obtained $42.9 \times 10^{-11}iea_0(-Q_W/N)$. Neither calculation includes structural radiation, the weak correlation potential, and normalization of states, effects which are included by us.

The $E1_{\text{PNC}}$ amplitude for the $6s\ ^2S_{1/2} \leftrightarrow 7s\ ^2S_{1/2}$ transition in Cs is about $0.9 \times 10^{-11}iea_0(-Q_W/N)$ [6]. Thus, the APNC effect in Ra^+ is larger by a factor close to 50. In heavy atoms, ANPC gets enhanced by the overall factor $K_r Z^2 Q_W(Z, N)$, where $Q_W \sim N \sim Z$, and K_r is a relativistic factor that depends on the nuclear charge and radius. This is the “faster-than- Z^3 law” [1], which implies that Ra^+ is favored over Cs by a factor of about 20. An additional factor of around 2 can be understood as follows. For Cs (and Fr) the S - S transition is used, for Ra^+ (and Ba^+) the S - D transition. Since the Z^0 -boson is very heavy, the weak interaction between electrons and the quarks in the nucleus has (almost) zero range. The overlap of the electrons with the nucleus is largest for the S states, and thus the mixing of the P -states into the S states gives the major contribution to $E1_{\text{PNC}}$. However, in Cs and Fr the initial and final S states contribute with opposite signs, which leads to a significant cancellation in $E1_{\text{PNC}}$. In fact, for Cs there are three dominant terms in the sum over the states, which add up to a total value that is half the size of the largest individual term [6].

The S - D transitions in Ba^+ and Ra^+ do not suffer from such a cancellation, since the contribution from the D -state to APNC is small. In Table II, we analyze which intermediate states contribute most to the total sum. Clearly, in contrast to the Cs S - S case, the sum is strongly dominated by one term: the contribution from the $7p\ ^2P_{1/2}$ state. These qualitative results are robust, they are consistent with the findings of Ref. [19], and they are, in fact, already borne out by a simple calculation with quantum-defect theory, analogous to Ref. [20]. This simple estimate gives for Cs, Fr, Ba^+ , and Ra^+ results accurate to some 10%; for Ra^+ we find $E1_{\text{PNC}} = 45(4) \times 10^{-11}iea_0(-Q_W/N)$.

In Table III, we present our results for the excitation energies, $E1$ transition amplitudes, and hyperfine constants for the relevant transitions and states in Ra^+ . We also list experimental values where available. For the excitation energies, we compare to the only available spec-

TABLE II: The contributions to the $E1_{\text{PNC}}$ from the different P -states (%).

| State | type | % | State | type | % |
|-----------------|-------|------|------------------|-----------|------|
| $6p\ ^2P_{1/2}$ | core | 8.7 | $8p\ ^2P_{1/2}$ | bound | -3.3 |
| $6p\ ^2P_{3/2}$ | core | -15 | $9p\ ^2P_{1/2}$ | bound | -0.7 |
| $7p\ ^2P_{1/2}$ | bound | 111 | $10p\ ^2P_{1/2}$ | continuum | -0.1 |
| $7p\ ^2P_{3/2}$ | bound | -2.6 | $11p\ ^2P_{1/2}$ | continuum | 1.1 |

TABLE III: Excitation energies, $E1$ transition amplitudes, and A_I/g_I for different low-lying states of Ra^+ .

| Transition | $7s\ ^2S_{1/2}$ $7p\ ^2P_{1/2}$ | $7s\ ^2S_{1/2}$ $7p\ ^2P_{3/2}$ | $6d\ ^2D_{3/2}$ $7p\ ^2P_{1/2}$ | $6d\ ^2D_{3/2}$ $7p\ ^2P_{3/2}$ |
|---|------------------------------------|------------------------------------|------------------------------------|------------------------------------|
| <i>Excitation energy</i> [cm^{-1}] | | | | |
| This work | 21509 | 26440 | 9734 | 14665 |
| Experiment [21] | 21351 | 26209 | 9267 | 14125 |
| <i>E1 transition amplitude</i> [a.u.] | | | | |
| This work | 3.31 | 4.58 | 3.68 | 1.56 |
| Ref. [19] | 3.223 | 4.477 | 3.363 | 1.504 |
| GTOs [22] | 3.28 | 4.54 | 3.64 | 1.54 |
| State | $7s\ ^2S_{1/2}$ | $7p\ ^2P_{1/2}$ | $7p\ ^2P_{3/2}$ | $6d\ ^2D_{3/2}$ |
| <i>Hyperfine interaction constant</i> (A_I/g_I) [MHz] | | | | |
| This work | 19689.37 | 3713.75 | 312.91 | 441.67 |
| Experiment [23] | 18772 | 3691 | 314.12 | - |

troscopy measurement [21], which dates back to 1933. For the $E1$ transition amplitudes, for which there are no experimental data, we list the results of Ref. [19] and of our previous work [22] using GTOs. Therein, the lifetimes of the metastable D -states were calculated to be $0.627(4)$ s for $6d\ ^2D_{3/2}$ and $0.297(4)$ s for $6d\ ^2D_{5/2}$.

Since the hyperfine structure is a good probe of the wave functions at the nucleus, we have, in order to estimate the accuracy of the $H_{\text{PNC}}^{\text{NSI}}$ matrix elements, calculated the ratio between the magnetic dipole hyperfine structure (A) and the nuclear gyromagnetic (g) constants, neglecting isotope effects, and compared these with experimental results for Ra^+ from ISOLDE [23, 24]. Our calculated value for $[A_I/g_I(7S_{1/2})A_I/g_I(7P_{1/2})]^{1/2}$ differs by 3% from the experimental value, which is a reasonable estimate for the dominant uncertainty in the atomic theory. Thus, our best value for the parity nonconserving $E1$ amplitude in Ra^+ is $E1_{\text{PNC}} = 46.4(1.4) \times 10^{-11}iea_0(-Q_W/N)$.

It appears feasible to push the accuracy of the atomic theory for Ra^+ to the sub-1% level. Improvements along several lines are in progress. The Breit interaction [25, 26] and QED corrections, which contribute around 1%, need to be included. The neutron-skin effect [27], which also contributes at the sub-1% level, has to be investigated. However, at the same time it is clear that experimental information to test the atomic theory is severely lacking. Not all relevant energy levels are known [21], there is no experimental information on the $E1$ transition strengths, nor on the lifetimes of the D -states. It is highly desirable to have more experimental data on the magnetic dipole and electric quadrupole hyperfine constants A and B for the various Ra^+ isotopes. The extraction of these constants [23, 24] is model dependent, and ideally one would like to use a single consistent *ab initio* framework for this.

TABLE IV: The properties of the isotopes of Ra^+ suitable for a single-ion APNC experiment. A is the mass number, I is the nuclear spin, and $\tau_{1/2}$ the half-life time.

| A | I | $\tau_{1/2}$ | Possible production reaction |
|-----|---------|--------------|---|
| 213 | $1/2^-$ | 2.74(6) min | $^{208}\text{Pb} + ^{12}\text{C} \rightarrow ^{213}\text{Ra} + 7\text{n}$ |
| 223 | $3/2^+$ | 11.43(5) d | $\text{p} + ^{232}\text{Th} \rightarrow ^{223}\text{Ra} + ^A\text{X} + a\text{n} + b\text{p}$ |
| 224 | 0^+ | 3.6319(23) d | $\text{p} + ^{232}\text{Th} \rightarrow ^{224}\text{Ra} + ^A\text{X} + a\text{n} + b\text{p}$ |
| 225 | $1/2^+$ | 14.9(2) d | $^{229}\text{Th} \rightarrow ^{225}\text{Ra} + \alpha$ |
| 226 | 0^+ | 1600(7) y | Commercially available |
| 227 | $3/2^+$ | 42.2(5) min | $\text{p} + ^{232}\text{Th} \rightarrow ^{227}\text{Ra} + ^A\text{X} + a\text{n} + b\text{p}$ |

At the TRI μ P facility, radium isotopes can be produced in fusion and evaporation or spallation reactions. The ions can be collected in a radio-frequency trap where they can be laser-cooled on the $7s\ ^2S_{1/2} \leftrightarrow 7p\ ^2P_{1/2}$ resonance line at 468 nm, with repumping via the $6d\ ^2D_{3/2} \leftrightarrow 7p\ ^2P_{1/2}$ transition at 1.08 μm , for which strong lasers are available. They will then be transferred to a miniature trap for the single-ion experiment, where techniques similar to Refs. [10, 11, 12] will be applied to perform the measurements. In particular, the $7s\ ^2S_{1/2} \leftrightarrow 7p\ ^2P_{3/2}$ and $6d\ ^2D_{5/2} \leftrightarrow 7p\ ^2P_{3/2}$ transitions at 381 nm and 801 nm, respectively, can be used for “shelving” [10].

A list of the Ra^+ isotopes suitable for a single-ion experiment is shown in Table IV. A half-life of the order of seconds is required for a high-precision single-ion experiment, but, on the other hand, it should not exceed a few days, so as to avoid long-lived radioactive contamination of the core equipment. Good candidates therefore are the odd isotopes $^{213}\text{Ra}^+$ and $^{227}\text{Ra}^+$, and the even isotope $^{224}\text{Ra}^+$. (Since the odd isotopes have a nonzero nuclear spin, the nuclear spin-dependent weak interaction will contribute to $E1_{\text{PNC}}$ [28]). The isotopes listed can all be produced at TRI μ P, and the experimental data required to constrain the atomic theory can be measured there with laser spectroscopy. Since multiple Ra^+ isotopes will be available, the possibility exists to measure APNC in a chain of isotopes, which can help to eliminate remaining uncertainties in the atomic theory [29].

In conclusion, Ra^+ appears to be an excellent candidate for an APNC experiment, since $E1_{\text{PNC}}$ is large, the required lasers are all at convenient wavelengths, and one can exploit the high-precision techniques of single-ion trapping. The atomic theory needed for the interpretation of the experiment could reach an accuracy better than 1%, but precise experimental data for the relevant atomic properties are mandatory to achieve such a benchmark. The prospects for APNC in Ra^+ as a precise test of the SM look promising.

Part of this work was supported by the Dutch Stichting voor Fundamenteel Onderzoek der Materie (FOM) under program 48 (TRI μ P) and project 06PR2499. The calculations were carried out using the Tera-flop Supercomputer in C-DAC, Bangalore.

- [1] M. A. Bouchiat and C. C. Bouchiat, Phys. Lett. B **48**, 111 (1974).
- [2] N. Fortson, Phys. Rev. Lett. **70**, 2383 (1993).
- [3] C. S. Wood, S. C. Bennett, D. Cho, B. P. Masterson, J. L. Roberts, C. E. Tanner, and C. E. Wieman, Science **275**, 1759 (1997).
- [4] S. C. Bennett and C. E. Wieman, Phys. Rev. Lett. **82**, 2484 (1999).
- [5] W. J. Marciano and J. L. Rosner, Phys. Rev. Lett. **65**, 2963 (1990).
- [6] J. S. M. Ginges and V. V. Flambaum, Phys. Rep. **637**, 63 (2004).
- [7] J. Guéna, M. Lintz, and M.-A. Bouchiat, Mod. Phys. Lett. A **20**, 375 (2005).
- [8] M. Lintz, J. Guéna, and M.-A. Bouchiat, Eur. Phys. J. A **32**, 525 (2007).
- [9] E. Gomez, L. A. Orozco, and G. D. Sprouse, Rep. Prog. Phys. **69**, 79 (2006).
- [10] T. W. Koerber, M. Schacht, W. Nagourney, and E. N. Fortson, J. Phys. B **36**, 637 (2003).
- [11] J. A. Sherman, T. W. Koerber, A. Markhotok, W. Nagourney, and E. N. Fortson, Phys. Rev. Lett. **94**, 243001 (2005).
- [12] T. W. Koerber, M. H. Schacht, K. R. G. Hendrickson, W. Nagourney, and E. N. Fortson, Phys. Rev. Lett. **88**, 143002 (2002).
- [13] G. P. Berg *et al.*, Nucl. Instr. Meth. A **560**, 169 (2006).
- [14] E. Traykov *et al.*, Nucl. Instr. Meth. A **572**, 580 (2007).
- [15] <http://www.kvi.nl/~radiumion>.
- [16] B. K. Sahoo, R. K. Chaudhuri, B. P. Das, and D. Mukherjee, Phys. Rev. Lett. **96**, 163003 (2006).
- [17] S. A. Blundell, J. Sapirstein, and W. R. Johnson, Phys. Rev. D **45**, 1602 (1992).
- [18] R. K. Chaudhuri, P. K. Panda, and B. P. Das, Phys. Rev. A **59**, 1187 (1999).
- [19] V. A. Dzuba, V. V. Flambaum, and J. S. M. Ginges, Phys. Rev. A **63**, 062101 (2001).
- [20] M. A. Bouchiat and C. C. Bouchiat, J. Phys. (Paris) **35**, 899 (1974); *ibid.*, **36**, 493 (1975).
- [21] E. Rasmussen, Z. Phys. **86**, 24 (1933).
- [22] B. K. Sahoo, B. P. Das, R. K. Chaudhuri, D. Mukherjee, R. G. E. Timmermans, and K. Jungmann, Phys. Rev. A **76**, 040504(R) (2007).
- [23] W. Neu, R. Neugart, E.-W. Otten, G. Passler, K. Wendt, B. Fricke, E. Arnold, H. J. Kluge, G. Ulm, and the ISOLDE collaboration, Z. Phys. D **11**, 105 (1989).
- [24] K. Wendt, S. A. Ahmad, W. Klempt, R. Neugart, E. W. Otten, H. H. Stroke, and the ISOLDE collaboration, Z. Phys. D **4**, 227 (1987).
- [25] A. Derevianko, Phys. Rev. Lett. **85**, 1618 (2000).
- [26] V. A. Dzuba, V. V. Flambaum, and M. S. Safronova, Phys. Rev. A **73**, 022112 (2006).
- [27] B. A. Brown, A. Derevianko, and V. V. Flambaum, arXiv.0804.4315v1 (2008).
- [28] K. P. Geetha, A. D. Singh, B. P. Das, and C. S. Unnikrishnan, Phys. Rev. A **58**, R16 (1998).
- [29] V. A. Dzuba, V. V. Flambaum, and I. B. Khriplovich, Z. Phys. D **1**, 243 (1986).